TOTAL KINETIC ENERGY MEASUREMENTS FOR SPONTANEOUS FISSION OF ^{255,256,258}Rf*

P. Mošať[a], S. Antalic[a], F.P. Hessberger[b,c], D. Ackermann[b,d]
B. Andel[a], M. Block[b,c,e], S. Hofmann[b,f], Z. Kalaninová[a,g]
B. Kindler[b], I. Kojouharov[b], M. Laatiaoui[b,c], B. Lommel[b]
A.K. Mistry[b,c], K. Nishio[b,h], J. Piot[d], B. Sulignano[b,i]
M. Vostinar[d,j]

[a]Department of Nuclear Physics and Biophysics
Comenius University in Bratislava, 84248 Bratislava, Slovakia
[b]GSI Helmholtzzentrum für Schwerionenforschung, GmbH
64291 Darmstadt, Germany
[c]Helmholtz-Institut Mainz, 55099 Mainz, Germany
[d]GANIL, 14076 Caen, France
[e]Johannes Gutenberg-Universität Mainz, 55128 Mainz, Germany
[f]Institut für Physik, Goethe-Universität Frankfurt, 60054 Frankfurt, Germany
[g]Laboratory of Nuclear Problems, JINR, 141980 Dubna, Russia
[h]JAEA, Tokai, Ibaraki 319-1195 Japan
[i]Irfu, CEA, Université Paris-Saclay, Gif-sur-Yvette, France
[j]University of Tennessee, Knoxville, Tennessee 37996, USA

(Received December 28, 2017)

Spontaneous fission of ^{255}Rf, ^{256}Rf and ^{258}Rf was studied at SHIP in GSI Darmstadt. The isotopes were produced in fusion–evaporation reactions ^{50}Ti + ^{207,208}Pb and ^{50}Ti + ^{209}Bi (compound nuclei ^{257}Rf, ^{258}Rf and ^{259}Db, respectively) and implanted into the focal plane detector of the SHIP setup. The deficit in the measured fragments energies was evaluated as a function of implantation depth of evaporation residues in the silicon detector. This correction was applied to obtain the mean total kinetic energies of ^{255}Rf, ^{256}Rf and ^{258}Rf.

DOI:10.5506/APhysPolB.49.605

1. Introduction

In the region of transfermium elements ($Z > 100$), spontaneous fission (SF) is the critical decay mode influencing the stability of nuclei [1]. The SF barrier dramatically decreases with the increasing proton number.

* Presented at the XXXV Mazurian Lakes Conference on Physics, Piaski, Poland, September 3–9, 2017.

According to the liquid-drop model, the fission barrier heights are close to zero for isotopes with $Z > 104$. These nuclei are stabilized mainly by microscopic effects resulting from the nuclear shell structure [2]. Systematic studies of SF properties in the very heavy element region are crucial for the understanding of these effects and determination of the possibility to produce the heaviest atomic nuclei. Up to now, only a few results with limited statistics of SF events with measured total kinetic energy (TKE) were obtained for rutherfordium ($Z = 104$) nuclei [3–6]. Theoretical calculations discuss the possibility of bimodal fission for even $^{254-260}$Rf isotopes, which should be noticeable in their TKE distributions [7]. Experimental studies of mass and TKE distributions confirmed the concept of bimodal fission in lighter nuclei [3, 4].

In this work, we present data on SF of rutherfordium isotopes obtained at SHIP, where fragment energies were measured by silicon detectors. For the evaluation of mean TKE release during the fission process, it is necessary to determine the correction to the deficit in the measured fragment energies obtained with silicon detectors calibrated by α-decay energies.

2. Experiment

Experiments aimed at the production of rutherfordium and dubnium ($Z = 105$) isotopes and investigations of their decay properties were carried out at GSI Darmstadt using the velocity filter SHIP. ^{50}Ti ions were accelerated by the UNILAC to energies from 225 to 243 MeV. The isotopes ^{255,256,258}Rf were produced in the fusion-evaporation reactions ^{50}Ti + ^{207,208}Pb and ^{50}Ti + ^{209}Bi. Targets of ^{207}PbS, ^{208}PbS and $^{209}Bi_2O_3$ of thicknesses 450 μg/cm^2, 450 μg/cm^2 and 463 μg/cm^2, respectively, were used. The evaporation residues ^{255}Rf and ^{256}Rf were created directly in the $1n$ and $2n$ evaporation channels from the compound nuclei. ^{258}Rf was produced indirectly, through the EC decay of ^{258}Db [8]. Reaction products were separated from the primary beam and other undesired nuclei by the velocity filter SHIP [9] and delivered to the detection setup. After passing through the time-of-flight system [10], they were implanted into the 16-strip position-sensitive silicon detector (STOP) placed at the focal plane of the separator [11]. Six detectors (BOX) of the same type and shape arranged in a "box" geometry were mounted just before the STOP detector to register escaping particles from the STOP into the backward hemisphere. A germanium clover detector (four crystals of 50–55 mm diameter and 70 mm length) was installed close behind the STOP detector for γ- and X-ray detection.

When registering SF of evaporation residues implanted in the STOP detector, three different cases can occur. Considering a 180° angle between the fission fragments, there is some probability (depending on the implantation

depth of evaporation residues) for one fragment to escape the STOP detector in the backwards direction. For the escaped fragment, there is about 80% probability to be detected in the BOX detector. These SF events are referred to as "STOP–BOX coincidences" (see Fig. 1 (a)). The remaining 20% of the escaped fragments leave the setup without being detected in the BOX detector (Fig. 1 (b)). The third group contains events with both fragments stopped in the STOP detector (Fig. 1 (c)) and thus they do not produce signal in the BOX detector. Therefore, fission events with one escaped fragment not registered by the BOX cannot be separated from the events with both fragments stopped in the STOP detector. We refer to both cases as "STOP–BOX anticoincidences".

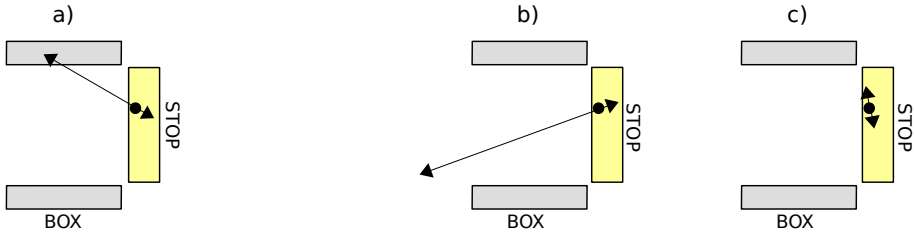

Fig. 1. Schematic view of STOP and BOX detectors registering fragments from SF of an implanted nucleus. Three different cases, depending on the direction of fragments can occur: (a) STOP–BOX coincidence with one fragment escaping to the BOX detector, (b) STOP–BOX anticoincidence with both fragments staying in the STOP detector, (c) STOP–BOX anticoincidence with one escaped fragment not registered by the BOX detector.

3. Correction for energy deficit in the measured TKE

When evaluating the $\langle \mathrm{TKE} \rangle$ using silicon detectors, the correction of the deficit in the measured energies is crucial. There are two main effects influencing the TKE measurements, discussed in previous studies performed at SHIP [12, 13]. First is the pulse-height defect (see *e.g.* Ref. [14]) due to non-ionizing interactions with atoms in the detector and recombination of electron–hole pairs. The pulse-height defect is negligible for light ions such as α particles (up to 1%) but becomes very important for heavy ions such as fission fragments (more than 10%). The energy calibration of the silicon STOP and BOX detectors was based on α-decay energies of implanted nuclei and, therefore, one has to correct the TKE for the pulse-height defect. The second effect is the strong dependence of the energy deficit on the implantation depth in the STOP detector, which, in our case, is usually few μm. The typical range of fission fragments in the silicon material is 10–20 μm, giving the opportunity for one fragment to escape. In the case of

STOP–BOX anticoincidences with one fragment escaping, the fission energy cannot be fully reconstructed. The presence of these events in the spectrum results in a low-energy tail. In the cases when fragments escape (for both STOP–BOX coincidences and anticoincidences), they pass through the dead layers of the STOP and possibly BOX detector under various angles, which also contributes to the energy deficit.

In order to evaluate the energy deficit, a calibration reaction ^{48}Ca + ^{206}Pb was performed to produce ^{252}No for which the value of $\langle$TKE$\rangle$ = 194.3 MeV is well-known from previous studies [4]. We measured the $\langle$TKE$\rangle$ of ^{252}No at six different implantation depths. The analysis for STOP–BOX coincidences was published previously [12], where the implantation depths were calculated with SRIM [15] and a linear fit was used for $\langle$TKE$\rangle$/implantation depth dependence. However, SRIM is able to calculate the energy losses and ranges only for isotopes up to uranium ($Z = 92$) and for heavier isotopes an extrapolation is necessary. Therefore, we decided to use LISE++ [16] in this work, due to its possibility to calculate the implantation depth directly for heavier nuclei. The cross-check was done with SRIM. In addition to previous works, we also evaluated the correction for STOP–BOX anticoincidences.

Considering that the reactions took place in the middle of the target, we calculated energy losses of ^{48}Ca projectiles in the first half of the target material (40 μg/cm^2 of C and 225 μg/cm^2 of ^{206}PbS) and energy losses of created evaporation residues of ^{252}No passing through the second half of the target (225 μg/cm^2 of ^{206}PbS and 10 μg/cm^2 of C), charge equilibration foil (30 μg/cm^2 of C) and 2 or 3 pairs of time-of-flight (TOF) detector foils (one foil consists of 30 μg/cm^2 of C). Mylar degrader foils were placed just before the detection setup to achieve various implantation depths. The resulting kinetic energies before entering the detector and the implantation depths of ^{252}No are shown in Table I. It should be noted that when evaporation residues are entering the silicon STOP detector, they pass through a 10 μg/cm^2 thick dead layer, where they lose about 0.21–0.28 MeV (calculated with LISE++ for 1–30 MeV evaporation residues of ^{252}No).

The analysis was done separately for the STOP–BOX anticoincident and coincident events. The results for STOP–BOX anticoincidences shown in Fig. 2 (a) exhibit a strong non-linear $\langle$TKE$\rangle$ dependence on the implantation depth. For higher implantation depths, the energy deficit decreases.

For implantations deeper than the range of a fission fragment, the energy deficit reaches its minimum and becomes constant. The measured $\langle$TKE$\rangle$ saturates to a constant maximal value and thus the obtained experimental points were fitted with a saturation-growth function.

In the case of STOP–BOX coincidences, the signals from both detectors were summed up to evaluate the TKE of fission event. The results are shown in Fig. 2 (b). The energy deficit also decreases with higher implantation

TABLE I

Kinetic energies and implantation depths of ^{252}No, calculated with SRIM [15] and LISE++ [16]. In the table columns, from left to right, thickness of degrader foils, number of time-of-flight foils, entering energies and implantation depths calculated with SRIM and LISE++ are shown.

Degrader foil thickness [μm]	TOF C foils [pcs]	SRIM		LISE++	
		energy [MeV]	impl. depth [μm]	energy [MeV]	impl. depth [μm]
0	4	32.9	5.69	31.8	5.67
0	6	30.8	5.37	29.5	5.31
0.72	6	26.7	4.68	25.5	4.69
2.15	6	18.6	3.31	18.0	3.45
4.16	6	10.3	2.01	8.5	1.7
6.59	6	1.1	0.2	0	0

depths and we again applied the fit with a saturation-growth function. The advantage of this approach is that we measure the energy of both fully detected fragments, however only at the cost of lower statistics of about 20% of all fission events.

For both STOP–BOX coincidences and anticoincidences, the energy deficit at a given implantation depth can be determined as the energy difference of the known $\langle \mathrm{TKE} \rangle$ of 194.3 MeV and the value from the experimental fit (Fig. 2) following:

$$\Delta E = (194.3 - \langle \mathrm{TKE} \rangle_{\mathrm{exp}})\ \mathrm{MeV}\,. \tag{1}$$

The implantation depths for ^{252}No calculated with SRIM and LISE++ (see Table I) are in a good agreement, even though the results from SRIM were obtained using an extrapolation of values for ^{238}U with the same kinetic energy-to-mass ratio of ^{252}No evaporation residues. On the other hand, we found some evident disagreements in directly (without extrapolation) calculated implantation depths for lighter nuclei. As an example, we did calculations of ranges for 40 MeV ^{238}U and ^{208}Pb in silicon. The results for ^{238}U are 6.83 μm and 6.77 μm for SRIM and LISE++, respectively. For the lighter nucleus ^{208}Pb, the difference in the calculated implantation depths becomes more significant, the values are 7.15 μm and 5.95 μm, respectively.

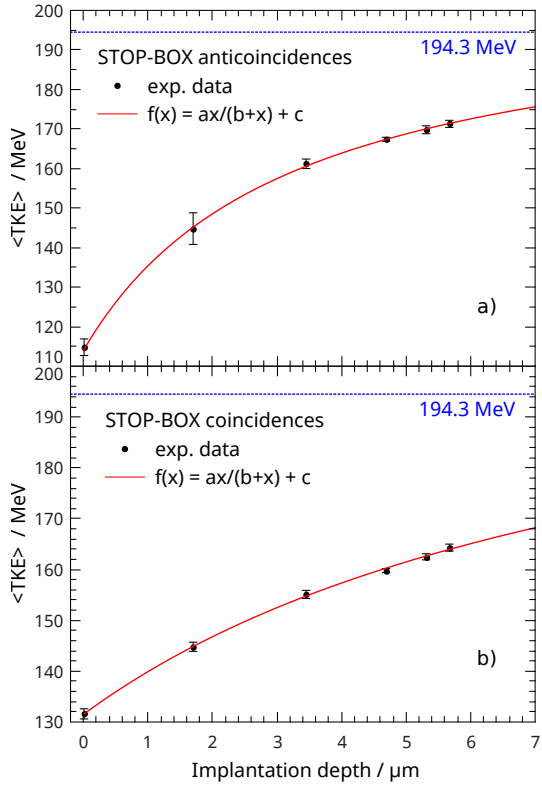

Fig. 2. Mean total kinetic energy of fragments from the fission of ^{252}No *vs.* implantation depth of evaporation residues in the STOP detector. (a) $\langle$TKE$\rangle$ of fission events from STOP detector in anticoincidence with BOX detector. (b) Fission events where the signal from STOP detector was in coincidence with the BOX detector. TKE of each fission event was reconstructed as a sum of signals from STOP and BOX. Dashed/blue line: $\langle$TKE$\rangle$ = 194.3 MeV of ^{252}No from Ref. [4]. Solid/red line: saturation-growth fit.

4. Results and discussion

Since the investigated Rf isotopes are close to ^{252}No, we applied the corrections evaluated above to correct the deficit in $\langle$TKE$\rangle$. The implantation depths of evaporation residues were 6.5–6.8 μm. This corresponds to energy corrections of 26–23 MeV for STOP–BOX coincidences and 22–19 MeV for anticoincidences.

We collected several hundreds of SF events for ^{255}Rf, ^{256}Rf and ^{258}Rf. The preliminary TKE spectra for each isotope are shown in Fig. 3. Depending on the type of event (STOP–BOX coincidences or anticoincidences) and also on implantation depth of evaporation residues, we applied the corresponding energy correction ΔE to the measured $\langle$TKE$\rangle$. The final results

of ⟨TKE⟩ from all collected fission events for each isotope are summarized in Table II. We obtained ⟨TKE⟩ of (199.5 ± 2.7) MeV for ^{255}Rf, which is in a good agreement with the value of (199 ± 3) MeV from [5], where ^{255}Rf was produced at SHIP indirectly by α decay of ^{259}Sg and ⟨TKE⟩ was corrected for the energy deficit using the method described in Ref. [12]. The ⟨TKE⟩ values of (198.7 ± 2.8) MeV for ^{256}Rf and (198.2 ± 3.0) MeV for ^{258}Rf are also in a good agreement with those previously measured: (198.9 ± 4.4) MeV and (197.6 ± 1.1) MeV [3], respectively.

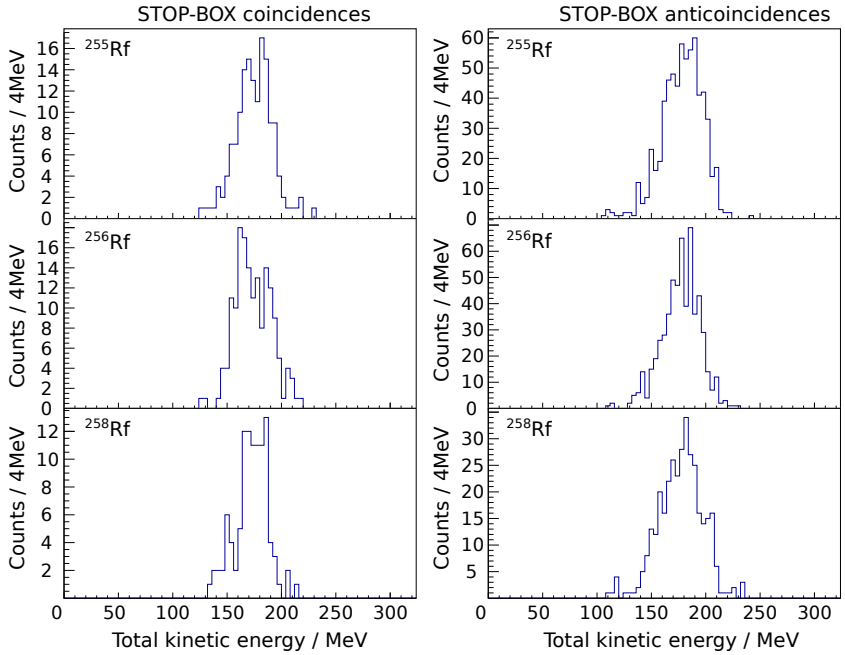

Fig. 3. Measured total kinetic energies of fragments from the fission of ^{255}Rf, ^{256}Rf and ^{258}Rf. Energy spectra were obtained from events of STOP–BOX coincidences (left) and anticoincidences (right).

TABLE II

Total kinetic energies evaluated in this work, compared to previous results. In the table columns, from left to right, isotope, ⟨TKE⟩ of all events obtained from STOP–BOX coincidences and anticoincidences, reference value of ⟨TKE⟩ and corresponding references are stated.

Isotope	$\langle \mathrm{TKE} \rangle_{\mathrm{exp}}$ [MeV]	$\langle \mathrm{TKE} \rangle_{\mathrm{ref}}$ [MeV]	Ref.
^{255}Rf	199.5 ± 2.7	199 ± 3	[5]
^{256}Rf	198.7 ± 2.8	198.9 ± 4.4	[3]
^{258}Rf	198.2 ± 3.0	197.6 ± 1.1	[3]

5. Conclusion

We determined the correction for the energy deficit in ⟨TKE⟩ measured by the detector setup at SHIP as a function of the implantation depth in the silicon STOP detector. A saturation-growth model was used to fit the data. The energy losses and ranges were calculated with LISE++ [16] and SRIM [15]. This study allows us to evaluate ⟨TKE⟩ of nuclei close to ^{252}No, such as rutherfordium isotopes ^{255}Rf, ^{256}Rf and ^{258}Rf. The results on ⟨TKE⟩ are in a good agreement with previous studies which supports the validity of our correction method.

This work was partly supported by the Slovak Research and Development Agency (contracts No. APVV-0105-10 and No. APVV-14-0524) and by the Slovak grant agency VEGA (contract No. 1/0532/17).

REFERENCES

[1] F.P. Heßberger, *Eur. Phys. J. A* **53**, 75 (2017).
[2] S.G. Nilsson *et al.*, *Nucl. Phys. A* **131**, 1 (1969).
[3] J.F. Wild *et al.*, *J. Alloy. Compd.* **213**, 86 (1994).
[4] E.K. Hulet, *Phys. At. Nucl.* **57**, 1099 (1994).
[5] S. Antalic *et al.*, *Eur. Phys. J. A* **51**, 41 (2015).
[6] A.I. Svirikhin *et al.*, *Phys. Part. Nucl. Lett.* **13**, 480 (2016).
[7] N. Carjan *et al.*, *Nucl. Phys. A* **942**, 97 (2015).
[8] F.P. Heßberger *et al.*, *Eur. Phys. J. A* **52**, 328 (2016).
[9] G. Münzenberg *et al.*, *Nucl. Instrum. Methods* **161**, 65 (1979).
[10] Š. Šáro *et al.*, *Nucl. Instrum. Methods Phys. Res. A* **381**, 520 (1996).
[11] S. Hofmann, G. Münzenberg, *Rev. Mod. Phys.* **72**, 733 (2000).
[12] K. Nishio *et al.*, *AIP Conf. Proc.* **891**, 71 (2007).
[13] S. Hofmann *et al.*, *Eur. Phys. J. A* **32**, 251 (2007).
[14] B.D. Wilkins *et al.*, *Nucl. Instrum. Methods* **92**, 381 (1971).
[15] J.F. Ziegler, M.D. Ziegler, J.P. Biersack, *Nucl. Instrum. Methods Phys. Res. B* **268**, 1818 (2010).
[16] O.B. Tarasov, D. Bazin, *Nucl. Instrum. Methods Phys. Res. B* **266**, 4657 (2008).